

---

# CONTINUAL PRUNE-AND-SELECT: CLASS-INCREMENTAL LEARNING WITH SPECIALIZED SUBNETWORKS

---

**Aleksandr Dekhovich**  
Delft University of Technology

**David M.J. Tax**  
Delft University of Technology

**Marcel H.F. Sluiter**  
Delft University of Technology

**Miguel A. Bessa \***  
Brown University

## ABSTRACT

The human brain is capable of learning tasks sequentially mostly without forgetting. However, deep neural networks (DNNs) suffer from catastrophic forgetting when learning one task after another. We address this challenge considering a class-incremental learning scenario where the DNN sees test data without knowing the task from which this data originates. During training, Continual-Prune-and-Select (CP&S) finds a subnetwork within the DNN that is responsible for solving a given task. Then, during inference, CP&S selects the correct subnetwork to make predictions for that task. A new task is learned by training available neuronal connections of the DNN (previously untrained) to create a new subnetwork by pruning, which can include previously trained connections belonging to other subnetwork(s) because it does not update shared connections. This enables to eliminate catastrophic forgetting by creating specialized regions in the DNN that do not conflict with each other while still allowing knowledge transfer across them. The CP&S strategy is implemented with different subnetwork selection strategies, revealing superior performance to state-of-the-art continual learning methods tested on various datasets (CIFAR-100, CUB-200-2011, ImageNet-100 and ImageNet-1000). In particular, CP&S is capable of sequentially learning 10 tasks from ImageNet-1000 keeping an accuracy around 94% with negligible forgetting, a first-of-its-kind result in class-incremental learning.<sup>2</sup> To the best of the authors' knowledge, this represents an improvement in accuracy above 20% when compared to the best alternative method.

**Keywords** continual learning, class-incremental learning, sparse network representation

## 1 Introduction

Despite significant progress, deep learning methods tend to forget old tasks while learning new ones. This is known as *catastrophic forgetting* in neural networks [1, 2]. In the conventional setting, a machine learning model has access to the entire training data at any point in time. Instead, in continual learning or lifelong learning [3] data for a given task comes in sequentially at a specific learning moment, and then new data associated to another task comes in at a different moment. Continual learning aims at creating deep learning models that do not forget previously learned tasks while being able to learn new ones, i.e. addressing catastrophic forgetting. Continual learning problems can be separated into two scenarios [4]: task-incremental learning (task-IL), where the task being solved is known both during training and inference; and class-incremental learning (class-IL) [5], where the task-ID is known only during training but unknown during testing. The class-IL problem is notably more challenging than task-IL. Addressing current challenges in class-IL brings the community one step closer to mimicking the abilities of the human brain.

There is evidence from neuroscience [6, 7, 8] that humans have special regions in the brain that are responsible for the recognition of specific patterns. Motivated by this observation, we propose a class-IL algorithm for image classification based on two steps: creating a subnetwork for a given task during training, and selecting a previously obtained

---

\*Corresponding author, e-mail: miguel\_bessa@brown.edu

<sup>2</sup>Code is available at: [https://github.com/adekhovich/continual\\_prune\\_and\\_select](https://github.com/adekhovich/continual_prune_and_select)

subnetwork during inference to make predictions. The first stage is achieved via iterative pruning that propagates input patterns through the network and eliminates the least useful connections. During inference, we first predict the current task when selecting the appropriate subnetwork from a small batch of test samples, and only then make a prediction with the selected subnetwork. We allow overlaps between subnetworks in order to induce knowledge transfer during training of new tasks. However, previously trained weights are not changed. Parameter update only occurs when training available neuron connections, which become part of a new subnetwork associated to the new task.

**Our contribution.** To the best of our knowledge, we propose for the first time a general strategy to create overlapping subnetworks of neuronal connections that share knowledge with each other for the class-IL scenario. In doing so, we achieve a strategy with negligible forgetting, unlike other works to date. Importantly, the choice of methods for subnetwork creation and for subnetwork selection *can be* different from the ones considered herein. Our goal is to propose a simple working paradigm for class-IL problems, where firstly some connections are assigned to a specific task during training that can then be selected during inference *without* knowing the task-ID.

This paper starts discussing state-of-the-art methods for continual learning, their differences and fundamental assumptions (Section 2). Then, the proposed CP&S strategy is presented (Section 3), and evaluated (Section 4) on class-incremental learning scenarios constructed from various datasets, including CIFAR-100 [9], ImageNet-100, ImageNet-1000 [10], and CUB-200-2011 [11]. In Section 5, additional experiments are provided showing limitations of CP&S approach and opening avenues for the conclusions and future directions (Section 6).

## 2 Related Work

**Class-incremental learning.** As previously mentioned, continual learning problems are usually classified according to whether or not the task-ID is available during inference. We focus on the class-IL scenario where the task ID is absent during inference, since it is the most realistic and challenging scenario of continual learning. All class-IL methods are usually divided into three categories [12]: *regularization* [13, 14, 15, 16, 17, 18], *rehearsal* [5, 19, 20, 21] and *architectural* [22, 23, 24].

Purely *regularization-based* methods introduce an additional term in the loss function to prevent forgetting. Some approaches [17, 13, 18, 25] estimate the importance of connections for a given task and penalize the model for gradient updates during training for the next tasks. Learning without forgetting (LwF) [14] adds a term in the loss function that penalizes changes in old output heads for new data, while training new output heads on new data. Regularization-based methods have the advantage of not storing past data in memory nor needing network expansion, but they perform worse compared to other approaches [4].

*Rehearsal* methods replay small amounts of old classes [5] or generate synthetic examples [26] to be able to predict previously seen classes. iCaRL uses the nearest class mean [27] (NCM) classifier together with fixed memory of old data to mitigate forgetting. Bias-correction methods [28, 19, 29] aim to tackle the tendency of class-IL algorithms to be biased towards classes of the last tasks, which arises due to class imbalance at the latest stages [4]. PODNet [21] has multiple terms in the loss function using old data from memory of a fixed size, penalizing signal deviations not only in the output layer but also in intermediate ones. The obvious limitation of rehearsal methods is the need to keep past data, which is often not desirable in practical applications due to privacy issues as mentioned by [30].

*Architectural* methods follow a different strategy where the network architecture is modified to avoid forgetting. For example, the Dynamically Expandable Network (DEN) [22] expands the network architecture in an online manner, increasing network capabilities, and introducing a regularization term to prevent forgetting. However, due to the expansion of the network, the final number of parameters is greater than for the original architecture, which increases the memory costs. Supermasks in Superposition (SupSup) [23] and SpaceNet [24] find subnetworks for every task. SpaceNet assigns parameters to one task only, without sharing knowledge between tasks which limits its allocation capabilities. SupSup uses a randomly weighted backbone [31] instead of pruning to obtain task-related subnetwork. During inference, SupSup predicts the correct subnetwork for the given test data, using all data points in the batch. In the provided experiments, the batch size is equal to 128 images which may not be applicable for real-life problems.

A Meta-Learning approach for class-IL is proposed by iTAML [32]. The algorithm for updating parameters for all old tasks also needs fixed sized memory, but iTAML uses a momentum based strategy for meta-updates to overcome catastrophic forgetting. At test stage, iTAML starts by predicting the task associated to that sample using a given test batch, and then adapts its parameters to the predicted task using data from fixed memory. Finally, with the adapted model and predicted task-ID, iTAML makes a prediction. Overall, iTAML uses samples from previous tasks to prevent forgetting, and the batch of test data to predict task-ID, making it the most demanding algorithm out of consideration. Also, the model adaptation to the predicted task makes it computationally more expensive than other state-of-the-art methods.

Table 1: Assumptions used by different types of class-IL methods (✓ means *yes*, ✗ means *no*; "bs" means batch size).

Methods	Replay old data	test bs > 1	Adaptation
SI, MAS, LwF, LwM, SpaceNet	✗	✗	✗
iCaRL, RPS-net, BiC, LUCIR, PODNet	✓	✗	✗
iTAML	✓	✓	✓
CP&S	✗	✓	✗

**Iterative pruning for Continual learning.** Typically, neural network pruning is used for model compression such that it reduces memory and computational costs. The pruning pipeline consist of three steps: network pretraining, deleting the least important connections or neurons based on some criterion, and network retraining. Iterative pruning is characterized by repeating the second and third steps several times. There are numerous approaches to pruning, namely magnitude pruning [33, 34, 35], data-driven pruning [36, 37, 38, 39] and sensitivity-based pruning [40, 41, 42, 43]. Iterative pruning has been recently applied in the context of task-IL but not in the more challenging class-IL scenario, where the task ID is not known *a priori*. Unsurprisingly, pruning has been shown to lead to simplified neural networks with a small fraction of the original parameters. This can facilitate the accumulation of knowledge for new tasks, as demonstrated by task-IL methods based on iterative pruning, namely PackNet [44] that uses magnitude connections pruning [33], and CLNP [45] that uses data-driven neurons pruning [37]. Piggyback [46] learns the mask for every task, as well as CPG [47] which also expands a network in the ProgressiveNet manner [48]. The performance of these algorithms is strong for task-IL, but they have the significant limitation of requiring to know the task-ID.

We are interested in developing a class-IL method that contains the benefits of iterative pruning connections to obtain sparse network representations, while being capable of selecting tasks without knowing the task-ID. To this effect, we developed a pruning strategy called NNrelief [39] that aims at leaving as many connections as possible available for future tasks, leading to sparser networks when compared to other pruning methods. The algorithm’s idea is to propagate signal through the network, compute a metric called importance score for each connection which estimates its contribution to the signal of the following neuron, and then prune the least contributing connections incoming to the neuron.

**Task selection.** Currently, there are few strategies for task selection in class-incremental learning. For example, iTAML [32] and SupSup [23] use similar ideas for task identification class-IL applied to image classification problems, and neither method uses pruning as a means to create space for new knowledge. The underlying assumption is that if a classifier network is well-trained, the highest output signal in the neuron of the output layer corresponds to the class belonging to the correct task. So, iTAML sums the largest output values of every task-related output in that layer over every test image in the batch, and then finds the layer with the highest total sum. SupSup relies on the entropy of the signal in each of the heads, in the hope that the model is confident in its prediction when it is in the correct head, meaning that the entropy of signal within the head should be smaller than in other heads. Note that both methods use batches of test samples to select the correct task: iTAML varies the batch size from 20 to 150 depending on the dataset, while SupSup uses 128 images in their experiments. A different strategy is pursued by Kim et al. [49], where an autoencoder is associated with a task during training. In the test stage, the reconstruction loss is computed for *every* autoencoder with the given test image, and the one with minimum reconstruction loss is chosen to make predictions. Subsequently, a classification model makes a prediction with the given predicted task-ID. It was shown that in the case of LwF [14] and LwM [15] this task-selection procedure improves classification accuracy. However, this task-selection approach requires training an autoencoder for every task which is impractical.

**Limitations of class-IL approaches.** State-of-the-art class-IL methods have simplified training by replaying old data [5, 21, 31, 19], doing inference with a batch of images to determine the current task [32, 23] and by performing adaptation before inference [32]. Table 1 summarizes these assumptions for each method. In rehearsal methods, examples of previous classes are stored (with fixed or growing memory), which makes them inappropriate when images should not be kept for a long time. Similarly, adaptation of a model for a given batch of test data before making a prediction (as in iTAML) is only possible when having examples in memory. Furthermore, the need for a significant number of images in a batch during inference arises from the difficulty of identifying the task-ID correctly with one image only. These can be strong model constraints when considering real-life applications.

### 3 Proposed Method

Our method is based on training a subnetwork for each given task, and then selecting the correct subnetwork when doing inference for new data with unknown task-ID. We start by training a regular neural network for a specific task,

iteratively pruning it to find a subnetwork with good performance. This creates a trained subnetwork capable of performing that particular task, leaving the remaining network free for future tasks. Importantly, when a new task comes in, the corresponding new subnetwork is found by iteratively pruning the entire original network – including all free neuronal connections *and* all existing subnetworks found for other tasks. This is possible by freezing the parameters of previously found subnetworks (avoiding to forget past tasks associated to the corresponding subnetworks), updating all the remaining parameters of the network, and then pruning the entire network until the corresponding subnetwork is found. This way, the new subnetwork can contain connections from other subnetworks but it does not affect their performance on past tasks because it did not update the parameters of *shared connections* – it only updated parameters of *unshared connections*. This allows to have transfer of knowledge from one task to another without forgetting.

The new strategy proposed herein can be implemented with different pruning algorithms to create each subnetwork, and with different task selection algorithms to find the correct subnetwork for inference. As long as the pruning and selection strategies have reasonable performance, we expect this strategy to outperform previous continual learning methods in the class-IL scenario because (1) it avoids forgetting if the task is selected correctly (unlike iTAML and SupSup); (2) it allows knowledge transfer among tasks (unlike SpaceNet); and (3) does not need to replay old data (unlike iCaRL, RPS-net, BiC, LUCIR and PODnet).

Without loss of generality, we use our recently developed NNrelief [39] pruning algorithm because it promotes sparser networks when compared to the state of the art, and it creates a renormalization effect in the network that distributes the importance of neuronal connections. Concerning task selection (in our case subnetwork selection), we considered different strategies, including the one proposed in the literature that applies to our method (see iTAML [32] and SupSup [23]).

Formally, denoting our classification network as  $\mathcal{N}$  and considering  $T$  tasks, then:

$$\mathcal{N} = \cup_{t=1}^T \mathcal{N}^t, \quad (1)$$

where  $\mathcal{N}^t$  is the subnetwork for task  $t$ , with  $t = 1, 2, \dots, T$ . Each subnetwork  $\mathcal{N}^t$  is found with our NNrelief pruning algorithm that determines the most important parts of the main network for solving a given task  $t$ . This algorithm estimates each connection contribution to the total signal of a receiving neuron when compared to the other connections that are incoming to that neuron. This contribution is computed by the *importance score* (IS) of every connection:

$$s_{ij}(\mathbf{x}_1, \mathbf{x}_2, \dots, \mathbf{x}_N) = \frac{\overline{|w_{ij}x_i|}}{\sum_{k=1}^m \overline{|w_{kj}x_k|} + |b_j|}, \quad (2)$$

for the input signal  $\mathbf{X} = \{\mathbf{x}_1, \dots, \mathbf{x}_N\}$  with  $N$  datapoints,  $\mathbf{x}_n = (x_{n1}, \dots, x_{nm}) \in \mathbb{R}^m$  for  $m$  neurons in that layer, where  $\overline{|w_{ij}x_i|} = \frac{1}{N} \sum_{n=1}^N |w_{ij}x_{ni}|$  and with  $w_{ij}$  being the weight of the connection between neurons  $i$  and  $j$ , where  $b_j$  is the bias in neuron  $j$ . Then NNrelief prunes the connections entering the neuron with the lowest contribution to the importance score whose sum is less than  $(1 - \alpha) \sum_{i=1}^m s_{ij}$ , where  $\alpha$  is the hyperparameter of the algorithm,  $0 \leq \alpha \leq 1$ . More details are given in the in Appendix A.1 and in our original article [39].

In the context of class-IL we receive datasets  $\mathbf{X}^1, \mathbf{X}^2, \dots, \mathbf{X}^T$  sequentially. The pruning algorithm then creates masks  $\mathbf{M}^1, \mathbf{M}^2, \dots, \mathbf{M}^T$  for every task  $t = 1, 2, \dots, T$ , where  $\mathbf{M}^t = (m_{ij}^t)_{i,j}$ ,

$$m_{ij}^t = \begin{cases} 1, & \text{if there is an active connection} \\ & \text{between neurons } i \text{ and } j, \\ 0, & \text{otherwise} \end{cases}$$

and corresponding importance scores  $S^1, S^2, \dots, S^T$ ,  $S^t = (s_{ij}^t)_{i,j}$ .

Once the subnetworks are created during training, selecting the correct subnetwork given a batch of test data becomes essential to do inference. In this article we define a test batch of size  $s$  as  $\mathbf{X}^{test} = \{\mathbf{x}_1^{test}, \mathbf{x}_2^{test}, \dots, \mathbf{x}_s^{test}\}$ , and can simplify the notation to cases where the fully connected part of the network consists of one layer, since we run all our experiments on ResNet architectures. However, there are no restrictions to apply this approach to any other type of architecture. We define the convolutional part for task  $t$  as  $\theta^t$ ,  $\theta^t : \mathbb{R}^{3 \times H \times W} \rightarrow \mathbb{R}^d$  ( $H, W$  are the height and width of an input image and  $d$  is the length of an output feature vector), and the fully connected layers as  $\varphi^t : \mathbb{R}^d \rightarrow \mathbb{R}^{num\_classes}$ .

Similarly to the selection of the pruning algorithm for subnetwork creation, we can also adopt different strategies to identify the correct subnetwork associated to a particular task. In order to establish a fair comparison with the literature, we focus on the *maximum output response* (maxoutput) strategy that is used by other methods (e.g. [32, 23]), but we also show that other task selection methods can lead to good results (see Supplementary Material for a strategy based on Importance Scores).

The maxoutput strategy for task prediction is simply formulated as:

$$t^* = \arg \max_{t=1,2,\dots,T} \sum_{i=1}^s \max \varphi^t(\theta^t(\mathbf{x}_i^{test})). \quad (3)$$

This does not require data storage. There are no memory costs associated to this prediction.

## 4 Experiments

We compare CP&S with different methods available in the literature. Aiming to establish a fair comparison, we use different measurements of accuracy during the learning process, namely *average multi-class accuracy* (ACC), *backward transfer metric* (BWT) [50] and *average incremental accuracy* (AIA) [5]. These metrics can be written assuming that a model learned  $T$  tasks and denoting  $R_{t_2,t_1}$  as the accuracy for task  $t_1$  after learning up to task  $t_2$  (inclusive, i.e.  $t_2 \geq t_1$ ):

$$\text{ACC}(T) = \frac{1}{T} \sum_{t=1}^T R_{T,t} \quad (4)$$

$$\text{BWT}(T) = \frac{1}{T-1} \sum_{t=1}^{T-1} R_{t,t} - R_{T,t} \quad (5)$$

$$\text{AIA}(T) = \frac{1}{T} \sum_{t=1}^T \text{ACC}(t) \quad (6)$$

The idea of the BWT is to measure the forgetting of the incremental-learning models, evaluating how much information about previous tasks is lost after learning a new one. We evaluate all methods using several class orderings to obtain robust results, as recommended in [4].

**Datasets.** We evaluate CP&S on three datasets: ImageNet-1000, including its subset ImageNet-100 [10]; CUB-200-2011 [11]; and CIFAR-100 [9]. We also consider different task construction scenarios. For completeness, the datasets are briefly described as follows:

- ImageNet-1000 consists of 1,281,167  $224 \times 224$  RGB images for training and 50,000 images for validation of 1000 classes. We split both ImageNet-100 and ImageNet-1000 in 10 incremental steps of equal size, similarly to the literature;
- CUB-200-2011 consists of 11,788  $224 \times 224$  RGB images of 200 classes with 5,994 training and 5,794 for testing images;
- CIFAR-100 consists of 60,000  $32 \times 32$  RGB images of 100 classes with 6k images per class. There are 50,000 training samples and 10,000 test samples;

We start our experiments with ImageNet-100 (the first 100 classes of the ImageNet-1000 dataset) and with CIFAR-100 before considering more challenging datasets such as ImageNet-1000 and CUB-200-2011. For all datasets, we use the ResNet-18 architecture, as considered by previous methods. For ImageNet-100/1000 datasets, we split them into 10 tasks of the same size (each task having 10 classes). We compare CP&S with other state-of-the-art models, namely LwF [14], iCaRL [5], EEIL [28], BiC [19], RPS-net [31] and iTAML [32]. In addition, we provide a comparison with the case of Finetuning, when no anti-forgetting actions are performed, and a network sequentially learns new tasks one by one.

**ImageNet-100.** Figure 1 shows that CP&S outperforms state-of-the-art methods for this dataset, even when considering two different optimizers – Stochastic Gradient Descent (SGD) and Adam [51]. We use a learning rate of 0.1 for SGD and 0.01 for Adam, dividing it by 10 on epochs 30 and 60, and we consider weight decay of  $10^{-4}$  for both optimizers. Figure 1a shows our predictions using a smaller batch size than iTAML – 20 samples instead of 50 – and compares them with other methods. Figure 1b clarifies the influence of considering different test batch sizes in CP&S method, where it is demonstrated that even when using 5 or 10 samples per batch we still perform better. The same figure also shows that when using Adam we identify the correct subnetwork in 100% of the cases because we reach the upper bound provided in the task-IL scenario, i.e. where the task-ID is known and subnetwork selection is not necessary. For SGD, we observe a slight drop in accuracy after task 8 compared to the task-IL scenario, although it

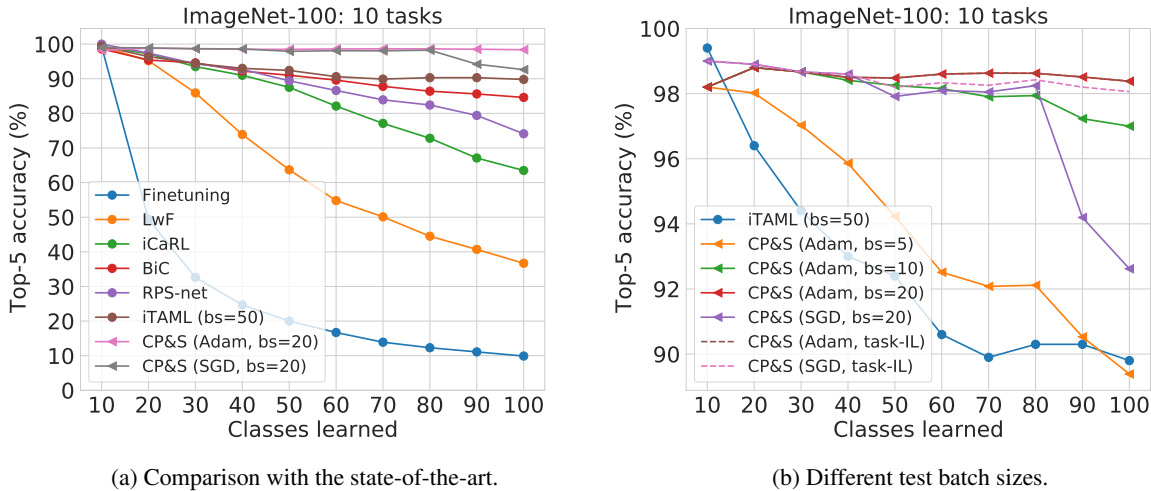


Figure 1: Results on ImageNet-100 and comparison with other approaches. Notation: "bs" refers to the test batch size; "task-IL" refers to task-IL scenario where the task-ID is known, providing an upper bound to the results. The pruning parameter of CP&S is  $\alpha_{conv} = 0.9$  for both optimizers, SGD and Adam. The class ordering is generated by seed 1993 (iCaRL seed).

still outperforms iTAML even though the latter uses 50 images for task identification and requires keeping images in memory. Overall, CP&S reaches 98.38% accuracy with Adam and 92.62% with SGD, translating into improvements for this dataset beyond 8% and 2.5% when compared to next best method, and even larger when compared to other methods after all classes are learned.

We note that using Adam [51] is advantageous for CP&S due to the higher level of sparsity that is produced after pruning with NNrelief when compared with other optimizers [39]. Note that pruning makes neuron connections available for creating new subnetworks associated to future tasks. If the number of available connections is small, then new subnetworks may not be sufficiently expressive to reach high accuracy for a given task. A similar effect is expected if the number of tasks is large, as shown in the next experiments for CIFAR-100.

**CIFAR-100.** Before considering more challenging datasets such as ImageNet-1000 and CUB-200-2011, we focus on CIFAR-100 where we split its 100 classes by a different number of tasks: 5, 10 and 20 tasks composed by 20, 10 and 5 classes, respectively. For iTAML we followed the original implementation with hyperparameters described in the paper including the test batch size equal to 20, and using *ResNet-18(1/3)* [50] which is a modified version of the standard ResNet-18 architecture where the number of filters is divided by three. For CP&S, we use Adam for training using 70 epochs and starting with learning rate 0.01 that is then divided by 5 every 20 epochs. We use  $\alpha_{conv} = 0.9$  and 3 pruning iterations as the pruning parameters of NNrelief.

Figure 2 shows that when considering 5 or 10 tasks CP&S significantly outperforms iTAML with the same batch size. However, for twenty tasks our performance drops sharply after the eleventh task, even in the ideal case where the task-ID is given (task-IL scenario). Despite being able to alleviate this drop by considering a larger test batch size, or by considering a different strategy for task (subnetwork) selection based on Importance Scores (see Appendix A.3), we observe this drop occurs approximately at the same number of tasks, independently of the class ordering used. Figure 3a provides an explanation to what occurs for the 20 tasks case by showing a heatmap with the task-selection accuracy by row for every task after a new task is learned. We also evaluate the prediction accuracy for each task when the task-ID is known (task-IL scenario), so that we can isolate the effect of not being able to appropriately select the subnetwork of interest for a given task and the effect of achieving low accuracy for a specific task. We observe that even in this case, the accuracy for each new task after the eleventh also drops (see Figure 3b). Therefore, our method performs well until we reach a saturation point when there are not enough neuron connections available to create a sufficiently large subnetwork to achieve high prediction accuracy for a new task. This is a logical conclusion, as one can only learn new tasks while sufficient neuronal connections remain available for training. Increasing the size of the original architecture eliminates this issue.

In addition, note that we do not keep data in memory (no replay), neither do we need to use adaptation to estimate the task before making a final prediction, unlike the methods reviewed above. We also use smaller test batch sizes than

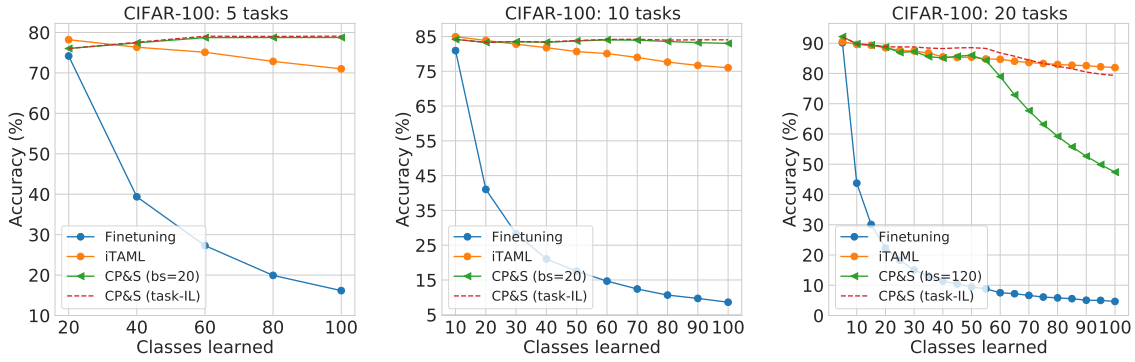
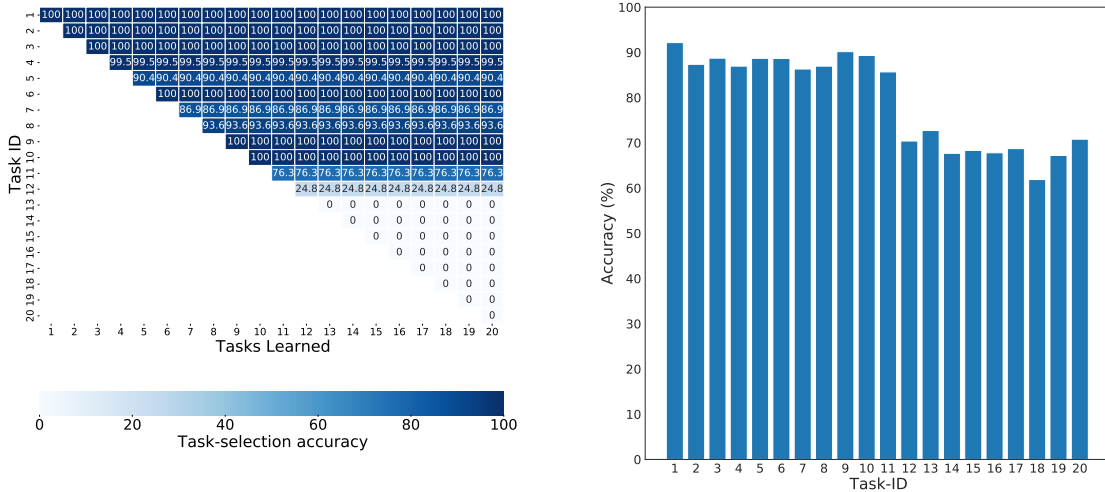


Figure 2: Comparison with iTAML on CIFAR-100 split in 5, 10 and 20 tasks. Notation: “bs” refers to the batch size during inference, “task-IL” refers to task-IL scenario where the task ID is known, providing an upper bound to the results. Five different class orderings are used.



(a) Maximum output response.

(b) Accuracy by task

Figure 3: CIFAR-100 divided into 20 tasks of 5 classes each. Task-selection accuracy with maxoutput (**left**) and accuracy by task (**right**).

iTAML, despite using the same task selection strategy. As shown by the next experiments, this conclusion holds for more challenging datasets.

**ImageNet-1000.** Focusing now on a more challenging dataset, we split ImageNet-1000 into 10 tasks of 100 classes. To evaluate CP&S, we train ResNet-18 with 90 epochs and SGD with a learning rate equal to 0.1 dividing it by 10 every 30 epochs. Figure 4a shows that CP&S performs better than the state of the art, exhibiting more than 20% higher accuracy than the next best method, which this time is BiC [19] instead of iTAML. We found this result to be particularly striking, since the prediction accuracy remains around 94% with virtually no forgetting for the first time in the literature, to the best of our knowledge. Figure 4b also shows results for different test batch sizes for determining the task-ID and corresponding subnetwork. Once again, a batch size of 20 provides a good trade-off between accuracy and sample size. Interestingly, prediction accuracy is better for CP&S method than others even when using only 5 test samples in the batch. With 20 images in the test batch we can almost reach the upper bound of the task-IL scenario, completely reaching it when using 50 images (i.e. identifying the task-ID correctly in 100% of the cases).

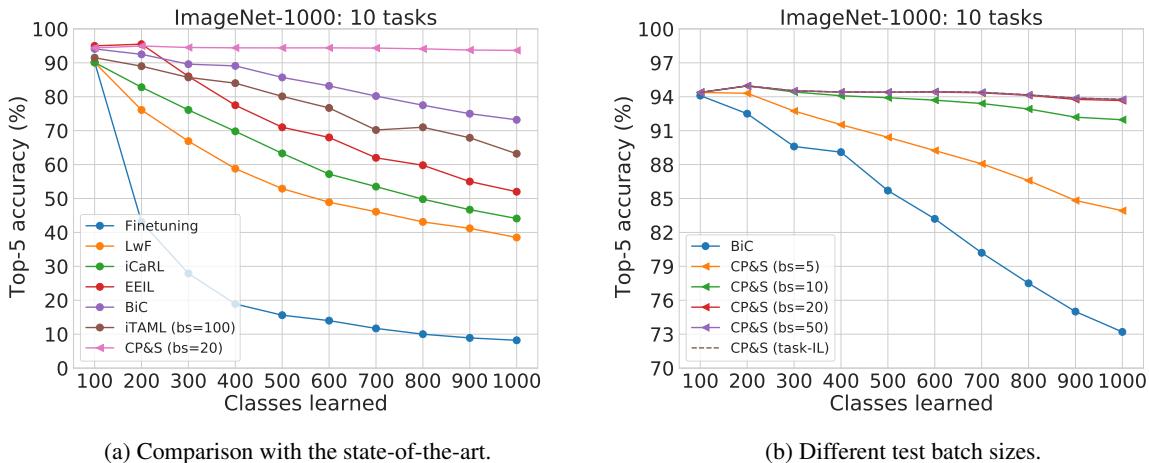


Figure 4: Results obtained for ImageNet-1000 dataset and comparison with other approaches. Notation: “bs” refers to the test batch size; “task-IL” refers to task-IL scenario (upper bound obtained when task ID is known). The pruning parameter is  $\alpha_{conv} = 0.9$  for CP&S. Class ordering is generated by seed 1993 (referring to iCaRL’s seed).

**CUB-200-2011.** We split CUB-200-2011 dataset into four tasks with 50 classes in each of the tasks. For testing, we take standard ResNet-18 pretrained on ImageNet-1000 [10] and fine-tuned with SGD. For iTAML, we also use pretrained weights and use the same hyperparameters for fine-tuning that are used in the original paper for other large-scale datasets. The pruning parameter for CP&S is  $\alpha_{conv} = 0.95$  and only one pruning iteration is used.

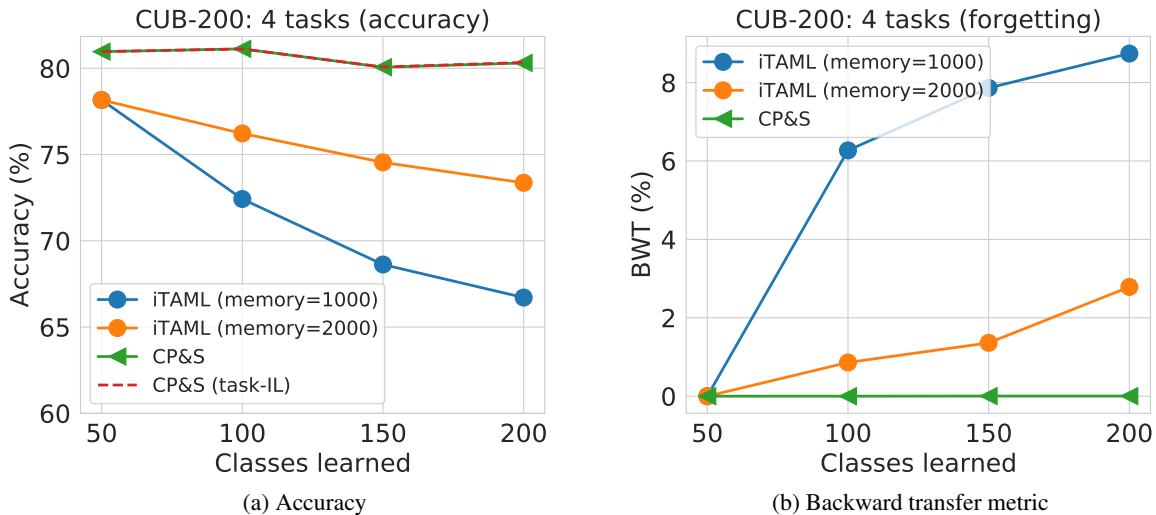


Figure 5: Comparison with iTAML on four tasks constructed from CUB-200-2011. Notation: “memory” is the number for images from previous tasks; “task-IL” refers to task-IL scenario as an upper-bound for our approach.

Figure 5 presents the accuracy and BWT history with 20 test images per batch, once again using maxoutput as the task-selection strategy. For 20 test images, it can be observed that CP&S once again exhibits almost no forgetting of information about previous tasks while learning new ones. However, iTAML even though it keeps 2000 images in memory, continuously forgets previous tasks. In addition, note that 2000 images represent 1/3 of the CUB-200-2011 dataset, and that we see a dramatic loss of performance for iTAML when using 1000 images (which is still 1/6 of all the images). In the case of 5 images per test batch, we obtain similar forgetting as iTAML with 2000 images in memory but still better forgetting metric than iTAML with 1000 images in memory. A more detailed comparison can be found in Appendix A.4, Figure 11.

In summary, CP&S outperformed the state-of-the-art for all datasets considered with the exception of CIFAR-100 when considering a large number of tasks. We demonstrate that we can perform better for small-scale and large-scale datasets (ImageNet-1000) where the second best methods are different. We considered scenarios where each task has a small or a large number of classes, including cases where there is a small number of training examples (CUB-200-2011) without keeping them in memory.

## 5 Further analysis

CP&S method’s performance degrades if there are too many tasks because the number of available neuron connections is not enough to create an expressive subnetwork and to select the correct task. This was shown for CIFAR-100 when considering 20 tasks (see Figure 2). In addition, there are scenarios where task selection during inference should be performed by a different strategy instead of maxoutput. For example, when there is an imbalanced number of classes within the tasks we note that using the modification of Importance Scores (IS) to select tasks is advantageous. Focusing on fully connected layers, for the given dataset  $\mathbf{X} = \{\mathbf{x}_1, \mathbf{x}_2, \dots, \mathbf{x}_s\}$  we can compute:

$$\hat{s}_{ij}^t = \overline{w_{ij} \cdot m_{ij}^t \cdot \theta_i^t(\mathbf{X})} = \begin{cases} \overline{w_{ij} \cdot \theta_i^t(\mathbf{X})}, & \text{if there is an active connection} \\ & \text{between neurons } i \text{ and } j \\ 0, & \text{otherwise,} \end{cases} \quad (7)$$

where  $\overline{w_{ij} \cdot \theta_i^t(\mathbf{X})} = \frac{1}{s} \sum_{k=1}^s w_{ij} \cdot \theta_i^t(\mathbf{x}_k)$  and  $\theta_i^t$  are the feature extractor layers of task  $t$ .

Suppose we have importance scores  $S^1, S^2, \dots, S^T$  obtained from the training set, we can estimate the importance scores of these connections based on  $\mathbf{X}^{test}$  for every subnetwork  $t = 1, 2, \dots, T$ , and denote these estimations as  $\hat{S}^1, \hat{S}^2, \dots, \hat{S}^T$ .

Assuming that importance scores should be similar for train and test data for the true task-ID, we can formulate the decisive rule as:

$$t^* = \arg \min_{t=1,2,\dots,T} \sqrt{\sum_{i,j} (s_{ij}^t - \hat{s}_{ij}^t)^2}, \quad (8)$$

where  $s_{ij}^t$  and  $\hat{s}_{ij}^t$  are the elements of matrices  $S^t$  and  $\hat{S}^t$  respectively,  $t = 1, 2, \dots, T$ .

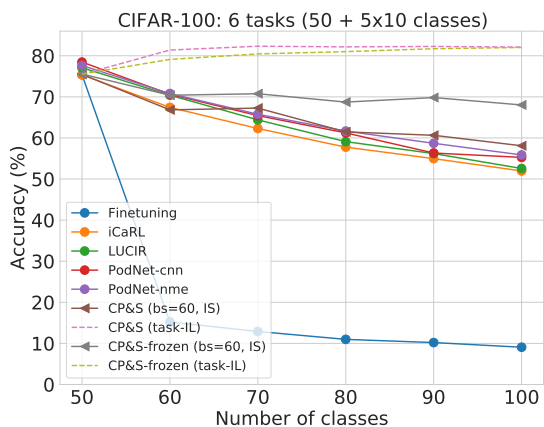
We consider the case where the first task consists of 50 classes, and 10 classes are in each of the following tasks, providing the comparison with iCaRL [5], LUCIR [19] and PODNet [21] (see Table 1 to recall different assumptions for each method). However, we also show that when using IS for task selection we require a larger batch size to improve task identification (60 test samples).

The maxoutput strategy does not work well in this case because most of the parameters are assigned to the first task (with 50 classes). As a result, this strategy predicts the first task when considering the last tasks for almost every batch, as shown in Appendix A.3, Figure 9.

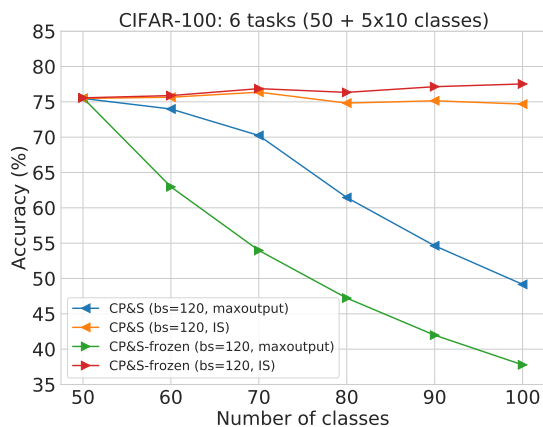
As a final comment, we also investigated an alternative solution when we have a first task that is significantly larger than the following ones. This can be solved by pretraining convolutional weights with the first task and training only the task-specific parts in the network. We denoted this last strategy as ‘‘CP&S-frozen’’ since we pretrain *all* convolutional parameters with the first 50 classes, and, for the next tasks we train task-related batch normalization parameters and the fully connected part that is task-specific by construction. So, in this last strategy each subnetwork consist of a common convolutional part (pretrained on the first task), batch normalization layers and output classification head. We present task-selection accuracy comparison between IS and maxoutput in Appendix A.3, Figure 10. We again observe poor performance for maximum output response strategy. The final results can be seen in Figure 6 and Table 2.

Table 2: Comparison between algorithms by average incremental accuracy and backward transfer metric at the end of all tasks. Mean values and standard deviation are computed using three different orderings.

Method	AIA (%)	BWT (%)
iCaRL	61.63 $\pm$ 0.25	12.77 $\pm$ 0.30
LUCIR	63.29 $\pm$ 0.36	10.09 $\pm$ 0.12
PODNet-CNN	64.56 $\pm$ 0.28	11.90 $\pm$ 0.04
PODNet-NME	65.07 $\pm$ 0.44	<b>1.18</b> $\pm$ 0.16
CP&S (bs=60, IS)	64.97 $\pm$ 4.23	11.68 $\pm$ 0.20
CP&S-frozen (bs=60, IS)	<b>70.55</b> $\pm$ 5.05	4.90 $\pm$ 2.35



(a) Comparison with state-of-the-art.

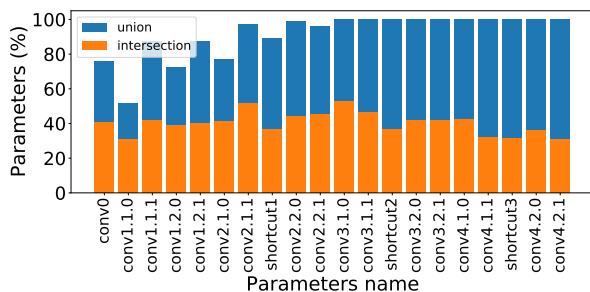


(b) IS and maxoutput with 120 images.

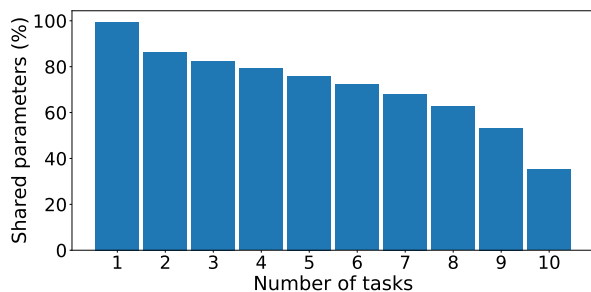
Figure 6: Accuracy history for ResNet-32 trained with CP&S and state-of-the-art. The pruning parameter is  $\alpha_{conv} = 0.9$  for CP&S strategy, and “task-IL” refers to the same upper bound mentioned in the previous figures. Three different class orderings are used.

We believe this knowledge transfer strategy might be interesting to explore in the future, where the first heads of the network specialize in selecting tasks and the deeper layers specialize in class prediction for each task.

**Knowledge transfer.** Let us explore how many parameters are used by the task (Figure 7). We consider the union and the intersection of all masks as sets. In Figure 7a we show how the union and intersection are distributed across parameters. From the union, we observe that the last layers are almost fully occupied in contrast to the first layers. From the intersection, it can be seen that a significant fraction of parameters are shared between each of the tasks across all layers. At the same time, about 85% are assigned to two and more tasks (Figure 7b). Notably, 35% of parameters are shared across all ten tasks, and about 50% of parameters are used for nine and more tasks. From these figures, we can conclude that almost all parameters are occupied at the end, having significant overlaps between subnetworks. However, looking at Figure 4, we see that performance remains stable, without drops. This allows us to conclude that subnetworks share knowledge between tasks, which helps to assimilate new patterns.



(a) The percentage of active parameters for union and intersection of masks by layer after the last task is learned.



(b) The percentage of shared parameters by the number of assigned tasks.

Figure 7: Visualization of employed masks and shared parameters for ResNet-18 on ImageNet-1000.

## 6 Conclusion

To overcome the problem of catastrophic forgetting while learning new tasks, we propose a continual learning algorithm that trains subnetworks for each task. During training of a task, weights are pruned and then fixed, such that future tasks cannot destroy the weights in this subnetwork, while still being able to use them for other subnetworks. During evaluation of new data, the correct task-ID and associated subnetwork has to be inferred from a small batch of samples. We describe existing task-prediction approaches and propose a new one based on the neural connection

strength. Although the task-ID needs to be inferred, no memory is needed to store examples from previous tasks, unlike alternative approaches. The main drawback of the current implementation of the CP&S strategy is the need to have a small batch of test data due to the difficulty of determining the correct task-ID – a limitation also observed in the best-performing methods in the literature. Notwithstanding, our work demonstrates that combining subnetwork creation and subnetwork selection methods into one paradigm provides a general approach to solve class-IL problems. We believe the proposed strategy can be further improved by developing better task-prediction strategies that do not need a batch of test data. CP&S outperforms all state-of-the-art methods on a variety of datasets. For ImageNet-1000, we show an improvement of more than 20% accuracy when compared to previous algorithms. Even though we apply CP&S to image classification tasks, no additional limitations are foreseen when applying it to other machine learning problems.

**Acknowledgement.** The authors would like to thank SurfSara for providing Snellius HPC cluster.

## References

- [1] Robert M French. Catastrophic forgetting in connectionist networks. *Trends in cognitive sciences*, 3(4):128–135, 1999.
- [2] Ian J Goodfellow, Mehdi Mirza, Da Xiao, Aaron Courville, and Yoshua Bengio. An empirical investigation of catastrophic forgetting in gradient-based neural networks. *arXiv preprint arXiv:1312.6211*, 2013.
- [3] Sebastian Thrun. Lifelong learning algorithms. In *Learning to learn*, pages 181–209. Springer, 1998.
- [4] Marc Masana, Xialei Liu, Bartłomiej Twardowski, Mikel Menta, Andrew D Bagdanov, and Joost van de Weijer. Class-incremental learning: survey and performance evaluation on image classification. *arXiv preprint arXiv:2010.15277*, 2020.
- [5] Sylvestre-Alvise Rebuffi, Alexander Kolesnikov, Georg Sperl, and Christoph H Lampert. icarl: Incremental classifier and representation learning. In *Proceedings of the IEEE conference on Computer Vision and Pattern Recognition*, pages 2001–2010, 2017.
- [6] Yulia Lerner, Christopher J Honey, Lauren J Silbert, and Uri Hasson. Topographic mapping of a hierarchy of temporal receptive windows using a narrated story. *Journal of Neuroscience*, 31(8):2906–2915, 2011.
- [7] Asieh Zadbood, Janice Chen, Yuan Chang Leong, Kenneth A Norman, and Uri Hasson. How we transmit memories to other brains: constructing shared neural representations via communication. *Cerebral cortex*, 27(10):4988–5000, 2017.
- [8] Peter R Huttenlocher. Morphometric study of human cerebral cortex development. *Neuropsychologia*, 28(6):517–527, 1990.
- [9] Alex Krizhevsky, Geoffrey Hinton, et al. Learning multiple layers of features from tiny images. 2009.
- [10] Jia Deng, Wei Dong, Richard Socher, Li-Jia Li, Kai Li, and Li Fei-Fei. Imagenet: A large-scale hierarchical image database. In *2009 IEEE conference on computer vision and pattern recognition*, pages 248–255. Ieee, 2009.
- [11] C. Wah, S. Branson, P. Welinder, P. Perona, and S. Belongie. The caltech-ucsd birds-200-2011 dataset. Technical Report CNS-TR-2011-001, California Institute of Technology, 2011.
- [12] Matthias Delange, Rahaf Aljundi, Marc Masana, Sarah Parisot, Xu Jia, Ales Leonardis, Greg Slabaugh, and Tinne Tuytelaars. A continual learning survey: Defying forgetting in classification tasks. *IEEE Transactions on Pattern Analysis and Machine Intelligence*, 2021.
- [13] Friedemann Zenke, Ben Poole, and Surya Ganguli. Continual learning through synaptic intelligence. In *International Conference on Machine Learning*, pages 3987–3995. PMLR, 2017.
- [14] Zhizhong Li and Derek Hoiem. Learning without forgetting. *IEEE transactions on pattern analysis and machine intelligence*, 40(12):2935–2947, 2017.
- [15] Prithviraj Dhar, Rajat Vikram Singh, Kuan-Chuan Peng, Ziyang Wu, and Rama Chellappa. Learning without memorizing. In *Proceedings of the IEEE/CVF Conference on Computer Vision and Pattern Recognition*, pages 5138–5146, 2019.
- [16] Xialei Liu, Marc Masana, Luis Herranz, Joost Van de Weijer, Antonio M Lopez, and Andrew D Bagdanov. Rotate your networks: Better weight consolidation and less catastrophic forgetting. In *2018 24th International Conference on Pattern Recognition (ICPR)*, pages 2262–2268. IEEE, 2018.
- [17] James Kirkpatrick, Razvan Pascanu, Neil Rabinowitz, Joel Veness, Guillaume Desjardins, Andrei A Rusu, Kieran Milan, John Quan, Tiago Ramalho, Agnieszka Grabska-Barwinska, et al. Overcoming catastrophic forgetting in neural networks. *Proceedings of the national academy of sciences*, 114(13):3521–3526, 2017.

- [18] Rahaf Aljundi, Francesca Babiloni, Mohamed Elhoseiny, Marcus Rohrbach, and Tinne Tuytelaars. Memory aware synapses: Learning what (not) to forget. In *Proceedings of the European Conference on Computer Vision (ECCV)*, pages 139–154, 2018.
- [19] Saihui Hou, Xinyu Pan, Chen Change Loy, Zilei Wang, and Dahua Lin. Learning a unified classifier incrementally via rebalancing. In *Proceedings of the IEEE/CVF Conference on Computer Vision and Pattern Recognition*, pages 831–839, 2019.
- [20] Eden Belouadah and Adrian Popescu. Il2m: Class incremental learning with dual memory. In *Proceedings of the IEEE/CVF International Conference on Computer Vision*, pages 583–592, 2019.
- [21] Arthur Douillard, Matthieu Cord, Charles Ollion, Thomas Robert, and Eduardo Valle. Podnet: Pooled outputs distillation for small-tasks incremental learning. In *Computer Vision—ECCV 2020: 16th European Conference, Glasgow, UK, August 23–28, 2020, Proceedings, Part XX 16*, pages 86–102. Springer, 2020.
- [22] Jaehong Yoon, Eunho Yang, Jeongtae Lee, and Sung Ju Hwang. Lifelong learning with dynamically expandable networks. *arXiv preprint arXiv:1708.01547*, 2017.
- [23] Mitchell Wortsman, Vivek Ramanujan, Rosanne Liu, Aniruddha Kembhavi, Mohammad Rastegari, Jason Yosinski, and Ali Farhadi. Supermasks in superposition. *Advances in Neural Information Processing Systems*, 2020.
- [24] Ghada Sokar, Decebal Constantin Mocanu, and Mykola Pechenizkiy. Spacenet: Make free space for continual learning. *Neurocomputing*, 439:1–11, 2021.
- [25] Arslan Chaudhry, Puneet K Dokania, Thalaiyasingam Ajanthan, and Philip HS Torr. Riemannian walk for incremental learning: Understanding forgetting and intransigence. In *Proceedings of the European Conference on Computer Vision (ECCV)*, pages 532–547, 2018.
- [26] Hanul Shin, Jung Kwon Lee, Jaehong Kim, and Jiwon Kim. Continual learning with deep generative replay. *Advances in Neural Information Processing Systems (NeurIPS)*, 2017.
- [27] Thomas Mensink, Jakob Verbeek, Florent Perronnin, and Gabriela Csurka. Metric learning for large scale image classification: Generalizing to new classes at near-zero cost. In *European Conference on Computer Vision*, pages 488–501. Springer, 2012.
- [28] Francisco M Castro, Manuel J Marín-Jiménez, Nicolás Guil, Cordelia Schmid, and Karteek Alahari. End-to-end incremental learning. In *Proceedings of the European conference on computer vision (ECCV)*, pages 233–248, 2018.
- [29] Yue Wu, Yinpeng Chen, Lijuan Wang, Yuancheng Ye, Zicheng Liu, Yandong Guo, and Yun Fu. Large scale incremental learning. In *Proceedings of the IEEE/CVF Conference on Computer Vision and Pattern Recognition*, pages 374–382, 2019.
- [30] Junting Zhang, Jie Zhang, Shalini Ghosh, Dawei Li, Serafettin Tasci, Larry Heck, Heming Zhang, and C-C Jay Kuo. Class-incremental learning via deep model consolidation. In *Proceedings of the IEEE/CVF Winter Conference on Applications of Computer Vision*, pages 1131–1140, 2020.
- [31] Jathushan Rajasegaran, Munawar Hayat, Salman Khan, Fahad Shahbaz Khan, and Ling Shao. Random path selection for incremental learning. *Advances in Neural Information Processing Systems*, 2019.
- [32] Jathushan Rajasegaran, Salman Khan, Munawar Hayat, Fahad Shahbaz Khan, and Mubarak Shah. itaml: An incremental task-agnostic meta-learning approach. In *Proceedings of the IEEE/CVF Conference on Computer Vision and Pattern Recognition*, pages 13588–13597, 2020.
- [33] Song Han, Jeff Pool, John Tran, and William J Dally. Learning both weights and connections for efficient neural networks. *arXiv preprint arXiv:1506.02626*, 2015.
- [34] Hao Li, Asim Kadav, Igor Durdanovic, Hanan Samet, and Hans Peter Graf. Pruning filters for efficient convnets. *arXiv preprint arXiv:1608.08710*, 2016.
- [35] Jonathan Frankle and Michael Carbin. The lottery ticket hypothesis: Finding sparse, trainable neural networks. *arXiv preprint arXiv:1803.03635*, 2018.
- [36] Hengyuan Hu, Rui Peng, Yu-Wing Tai, and Chi-Keung Tang. Network trimming: A data-driven neuron pruning approach towards efficient deep architectures. *arXiv preprint arXiv:1607.03250*, 2016.
- [37] Zehao Huang and Naiyan Wang. Data-driven sparse structure selection for deep neural networks. In *Proceedings of the European conference on computer vision (ECCV)*, pages 304–320, 2018.
- [38] Jian-Hao Luo, Jianxin Wu, and Weiyao Lin. Thinet: A filter level pruning method for deep neural network compression. In *Proceedings of the IEEE international conference on computer vision*, pages 5058–5066, 2017.

- [39] Aleksandr Dekhovich, David MJ Tax, Marcel HF Sluiter, and Miguel A Bessa. Neural network relief: a pruning algorithm based on neural activity. *arXiv preprint arXiv:2109.10795*, 2021.
- [40] Yann LeCun, John S Denker, and Sara A Solla. Optimal brain damage. In *Advances in neural information processing systems*, pages 598–605, 1990.
- [41] Babak Hassibi, David G Stork, and Gregory J Wolff. Optimal brain surgeon and general network pruning. In *IEEE international conference on neural networks*, pages 293–299. IEEE, 1993.
- [42] Babak Hassibi and David G Stork. *Second order derivatives for network pruning: Optimal brain surgeon*. Morgan Kaufmann, 1993.
- [43] Vadim Lebedev and Victor Lempitsky. Fast convnets using group-wise brain damage. In *Proceedings of the IEEE Conference on Computer Vision and Pattern Recognition*, pages 2554–2564, 2016.
- [44] Arun Mallya and Svetlana Lazebnik. Packnet: Adding multiple tasks to a single network by iterative pruning. In *Proceedings of the IEEE conference on Computer Vision and Pattern Recognition*, pages 7765–7773, 2018.
- [45] Siavash Golkar, Michael Kagan, and Kyunghyun Cho. Continual learning via neural pruning. *arXiv preprint arXiv:1903.04476*, 2019.
- [46] Arun Mallya, Dillon Davis, and Svetlana Lazebnik. Piggyback: Adapting a single network to multiple tasks by learning to mask weights. In *Proceedings of the European Conference on Computer Vision (ECCV)*, pages 67–82, 2018.
- [47] Ching-Yi Hung, Cheng-Hao Tu, Cheng-En Wu, Chien-Hung Chen, Yi-Ming Chan, and Chu-Song Chen. Compacting, picking and growing for unforgetting continual learning. *Advances in Neural Information Processing Systems*, 32, 2019.
- [48] Andrei A Rusu, Neil C Rabinowitz, Guillaume Desjardins, Hubert Soyer, James Kirkpatrick, Koray Kavukcuoglu, Razvan Pascanu, and Raia Hadsell. Progressive neural networks. *arXiv preprint arXiv:1606.04671*, 2016.
- [49] Eun Sung Kim, Jung Uk Kim, Sangmin Lee, Sang-Keun Moon, and Yong Man Ro. Class incremental learning with task-selection. In *2020 IEEE International Conference on Image Processing (ICIP)*, pages 1846–1850. IEEE, 2020.
- [50] David Lopez-Paz and Marc’Aurelio Ranzato. Gradient episodic memory for continual learning. *Advances in neural information processing systems*, 30:6467–6476, 2017.
- [51] Diederik P Kingma and Jimmy Ba. Adam: A method for stochastic optimization. *arXiv preprint arXiv:1412.6980*, 2014.

## A Appendix

### A.1 NNrelief details

For the incoming signal  $\mathbf{X} = \{\mathbf{x}_1, \mathbf{x}_2, \dots, \mathbf{x}_N\}$  with  $N$  datapoints  $\mathbf{x}_n = (x_{n1}, \dots, x_{nm_1}) \in \mathbb{R}^{m_1}$ , NNrelief computes the importance scores:

$$s_{ij}(\mathbf{x}_1, \mathbf{x}_2, \dots, \mathbf{x}_N) = \frac{\overline{|w_{ij}x_i|}}{\sum_{k=1}^{m_1} \overline{|w_{kj}x_k|} + |b_j|}, \quad (9)$$

where  $\overline{|w_{ij}x_i|} = \frac{1}{N} \sum_{n=1}^N |w_{ij}x_{ni}|$  and  $\mathbf{W} = (w_{ij}) \in \mathbb{R}^{m_1 \times m_2}$  is a corresponding weight matrix,  $\mathbf{b} = (b_1, b_2, \dots, b_{m_2})^T \in \mathbb{R}^{m_2}$  is a bias vector. Importance score for the bias of the neuron  $j$  is  $s_{m_1+1,j} = \frac{|b_j|}{\sum_{k=1}^{m_1} \overline{|w_{kj}x_k|} + |b_j|}$ .

The sketch of NNrelief algorithm for some fixed neuron  $j$  in the following layer is:

1. Choose  $\alpha \in (0, 1)$  – the amount of connections’ importance that we want to keep relatively to the total importance of the connections coming to the neuron  $j$ .
2. Compute importance scores  $s_{ij}$  for all connections to the neuron  $j$ ,  $i = 1, 2, \dots, m_1 + 1$ .
3. Sort importance scores  $s_{ij}$  for fixed neuron  $j$ .
4. For the sorted importance scores  $\hat{s}_{ij}$  find minimal  $p \leq m_1 + 1$  such that  $\sum_{i=1}^p \hat{s}_{ij} \geq \alpha$ .
5. Prune connections with the importance score  $s_{ij} < \hat{s}_{pj}$  for all  $i \leq m_1 + 1$  and fixed  $j$ .

## A.2 Importance scores (IS)

Instead of the maxoutput strategy we can consider alternatives to selecting subnetworks. For example, we can use Importance scores (IS). Focusing on fully connected layers and assuming we have importance scores  $S^1, S^2, \dots, S^T$  obtained from the training set, we can estimate the importance scores of these connections based on  $\mathbf{X}^{test}$ :

$$\hat{s}_{ij} = \overline{w_{ij} \cdot m_{ij}^t \cdot \theta_i^t(\mathbf{X}^{test})} = \begin{cases} \overline{w_{ij} \cdot \theta_i^t(\mathbf{X}^{test})}, & \text{if there is an active connection} \\ & \text{between neurons } i \text{ and } j \\ 0, & \text{otherwise,} \end{cases}, \quad (10)$$

where  $\overline{w_{ij} \cdot \theta_i^t(\mathbf{X}^{test})} = \frac{1}{s} \sum_{k=1}^s w_{ij} \cdot \theta_i^t(\mathbf{x}_k^{test})$ , and denote these estimations as  $\hat{S}^1, \hat{S}^2, \dots, \hat{S}^T$ . Assuming that importance scores should be similar for train and test data for the true task-ID, we can formulate the decisive rule as:

$$t^* = \arg \min_{t=1,2,\dots,T} \sqrt{\sum_{i,j} (s_{ij}^t - \hat{s}_{ij}^t)^2}, \quad (11)$$

where  $s_{ij}^t$  and  $\hat{s}_{ij}^t$  are the elements of matrices  $S^t$  and  $\hat{S}^t$  respectively,  $t = 1, 2, \dots, T$ .

## A.3 Different task selection strategies on CIFAR-100

We present CP&S results with different test batch sizes and task-selection strategies (see Figure 8).

## A.4 CUB-200-2011 additional comparison

In this section we provide an additional comparison for ResNet-19 on CUB-200-2011 dataset using 5 an 20 test images per batch to predict the task-ID.

## A.5 ImageNet-100/1000 results

For ImageNet-100/1000 we present exact numbers from which the plots are constructed for CP&S (see Table 3 and Table 4).

Table 3: ImageNet-100 results with different test batch sizes and task-IL scenario trained with SGD and Adam.

optimizer	batch size	1	2	3	4	5	6	7	8	9	10
Adam	20	98.2	98.8	98.67	98.5	98.48	98.6	98.63	98.63	98.5	98.38
	10	98.2	98.8	98.67	98.41	98.25	98.15	97.9	97.94	97.23	97.0
	5	98.2	98.02	97.03	95.86	94.23	92.51	92.08	92.12	90.53	89.39
	task-IL	98.2	98.8	98.67	98.5	98.48	98.6	98.63	98.63	98.5	98.38
SGD	20	99.0	98.9	98.67	98.6	97.9	98.09	98.05	98.25	94.2	92.62
	task-IL	99.0	98.9	98.67	98.6	98.2	98.33	98.26	98.425	98.2	98.06

Table 4: ImageNet-1000 results with different test batch sizes and task-IL scenario trained with SGD.

optimizer	batch size	1	2	3	4	5	6	7	8	9	10
SGD	50	94.38	94.96	94.52	94.42	94.4	94.45	94.4	94.16	93.88	93.77
	20	94.38	94.96	94.52	94.42	94.4	94.4	94.34	94.12	93.77	93.66
	10	94.38	94.96	94.42	94.09	93.91	93.7	93.40	92.92	92.19	91.97
	5	94.38	94.31	92.74	91.53	90.41	89.24	88.07	86.59	84.82	83.92
	task-IL	94.38	94.96	94.52	94.42	94.4	94.45	94.4	94.16	93.88	93.77

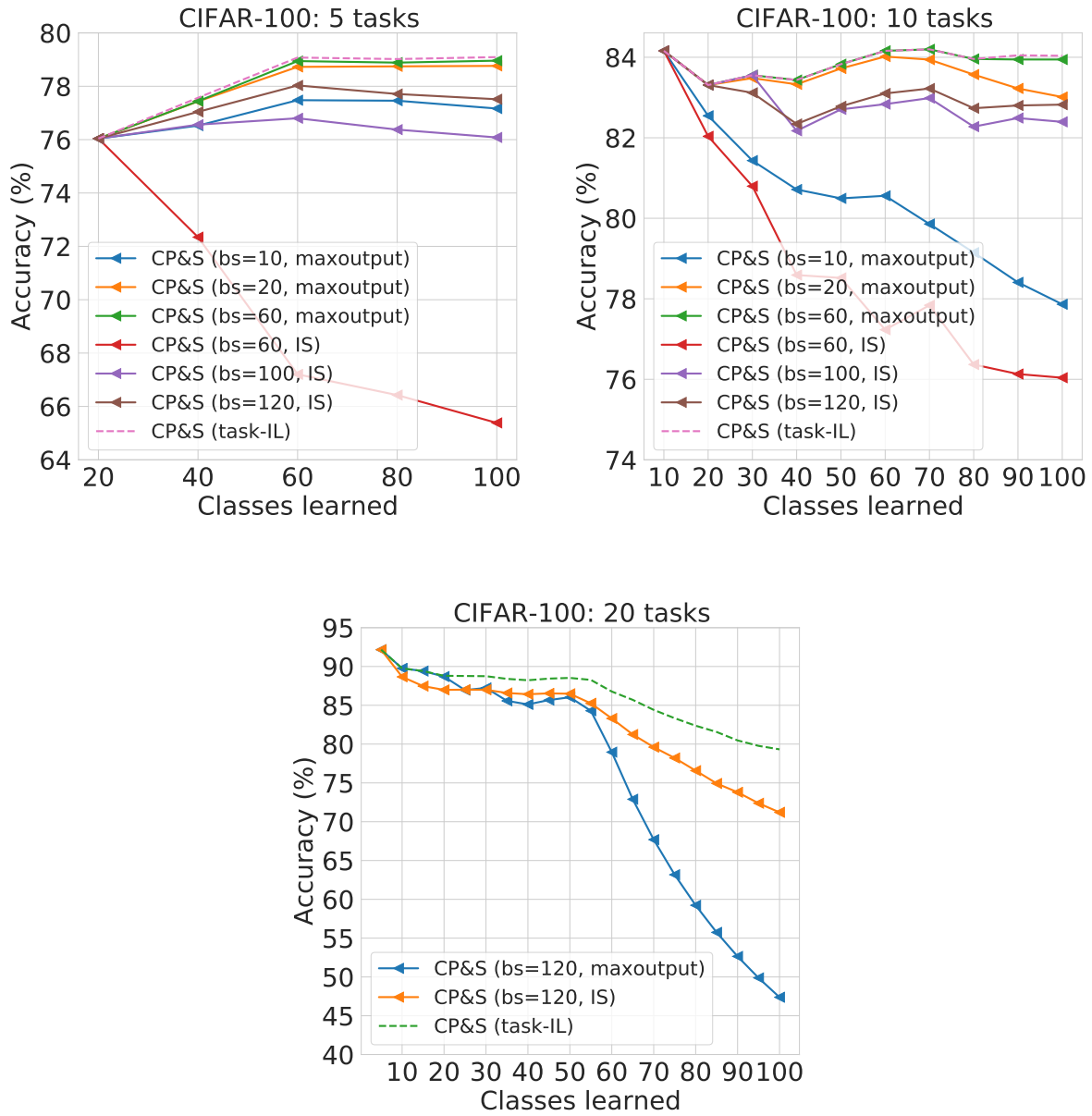
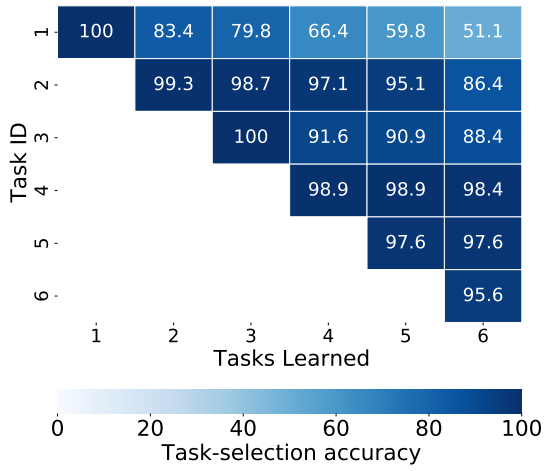
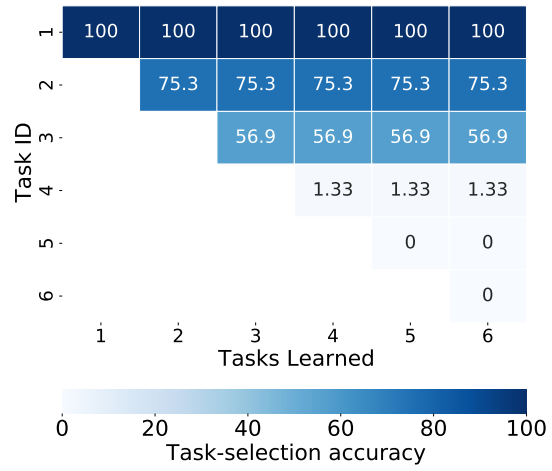


Figure 8: The performance of CP&S with different batch sizes and task-selection strategies.

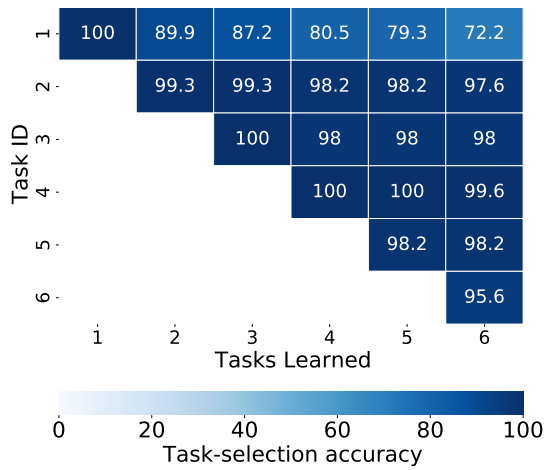


(a) CP&S (IS)

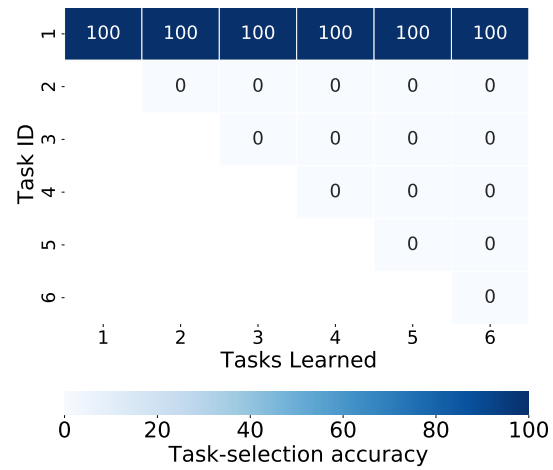


(b) CP&S (maxoutput)

Figure 9: Task-selection accuracy using Importance Scores (IS) as opposed to maxoutput on CIFAR-100 with class imbalance (50 classes in the first task and 10 classes in each of the following five tasks) for CP&S. The test batch size is 60 images in both cases.

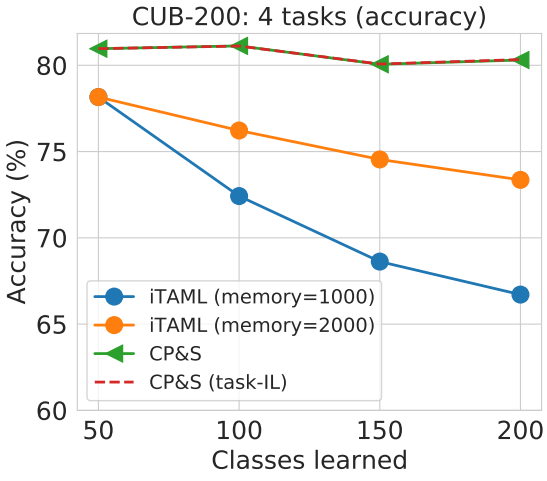


(a) CP&S-frozen (IS)

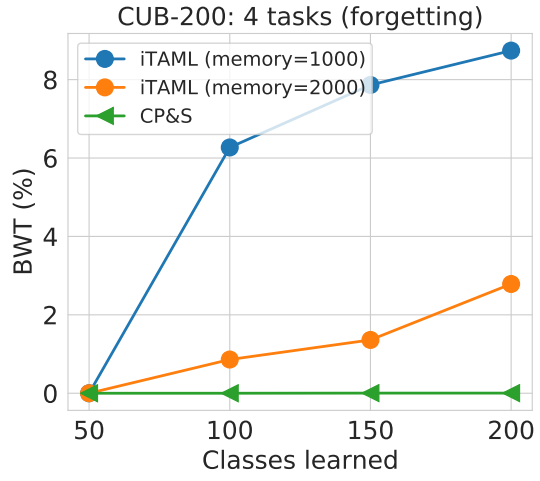


(b) CP&S-frozen (maxoutput)

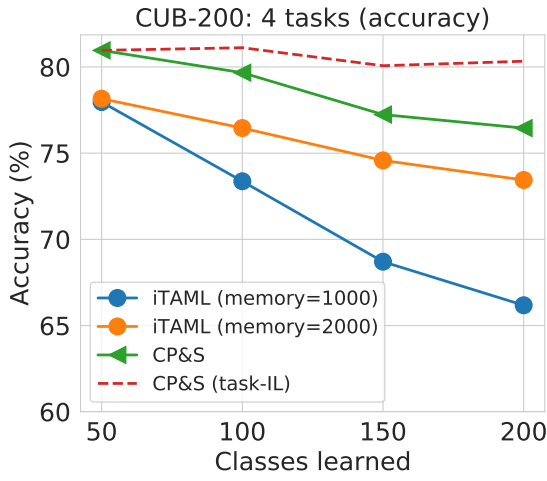
Figure 10: Task-selection accuracy using Importance Scores (IS) as opposed to maxoutput on CIFAR-100 with class imbalance (50 classes in the first task and 10 classes in each of the following five tasks) for CP&S-frozen. The test batch size is 60 images in both cases.



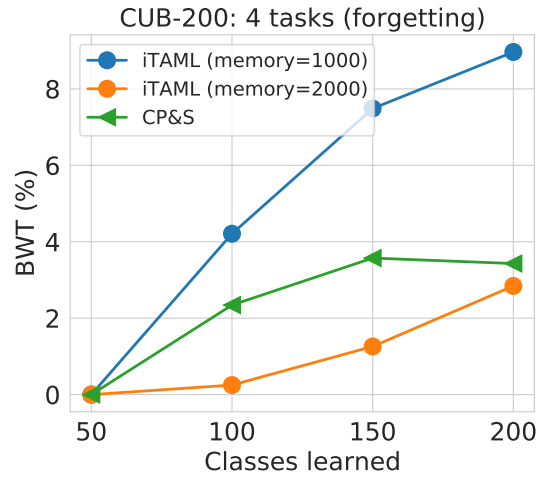
(a) Accuracy, test batch size = 20



(b) BWT, test batch size = 20



(c) Accuracy, test batch size = 5



(d) BWT, test batch size = 5

Figure 11: Comparison with iTAML on four tasks constructed from CUB-200-2011. Notation: “memory” is the number for images from previous tasks; “task-IL” refers to task-IL scenario as an upper-bound for CP&S.